Articles

Rotational Isomerism of a Phoban-Derived First-Generation Grubbs Catalyst

Catherine L. Dwyer,*,† Megan M. Kirk,† Wolfgang H. Meyer,*,†
Werner Janse van Rensburg,† and Grant S. Forman‡

Sasol Technology Research & Development, P.O. Box 1, Sasolburg 1947, South Africa, and Sasol Technology Research Laboratory, Sasol Technology (UK) Limited, St Andrews, Purdie Building, North Haugh, University of St Andrews, Fife, KY16 9ST, St Andrews, Scotland, United Kingdom

Received December 19, 2005

A ruthenium carbene complex bearing a bicyclic phosphine ligand instead of tricyclohexylphosphine of the otherwise identical first-generation Grubbs catalyst exhibits only a very broad singlet in the ^{31}P NMR at room temperature instead of the expected sharp signal. For this complex as well as for similar derivatives, low-temperature NMR experiments and DFT calculations proved the existence of rotational isomers with the employed unsymmetrical bicyclic phosphine ligand. Such rotational isomers cannot be observed for the first- and second-generation Grubbs catalysts, due to the symmetrical nature of their ligands.

Introduction

Ruthenium alkylidene complexes, commonly known as Grubbs catalysts, have become increasingly important in the area of metathesis chemistry.[1,2] The catalyst development has shifted from the bis(phosphine) first-generation catalysts **1** toward the highly active second-generation catalysts **2** based on N-heterocyclic carbene ligands (mes = 2,4,6-trimethylphenyl) (Figure 1).[3] The higher activity of complex **2** is not a simple function of ligand basicity but, rather, a combination of electronic and steric effects which influence the dissociation of a phosphine ligand as well as the ratio of olefin to phosphine coordination as important steps of the mechanistic cycle.[3j] The reason for the higher stability and lifetime of such compounds as compared to those of **1** was investigated under catalytic conditions[4a] but is generally much less understood, due to a variety of possible decomposition pathways, including bimolecular decomposition[4b] and CH activation of the ligand moiety.[4c] The second-generation catalysts generally exhibit lower selectivities toward desired primary metathesis products, due to double-bond isomerization and subsequent secondary metathesis product formation.[5] Limitations on the steric bulk and electronic properties seem to be limiting the scope for further improvement of these systems.[6] Focusing on the further development of first-generation catalysts[7] with monodentate phosphine ligands in-house expertise in the area of phosphine-modified cobalt-catalyzed hydroformylation[8] provided a basis, since those phosphines covered the requirements of ligand basicity and steric bulk for metathesis.

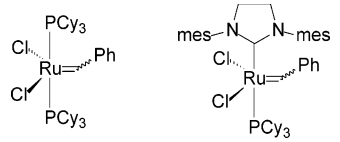

1 **2**

Figure 1. Grubbs first- (**1**) and second-generation catalysts (**2**).

The initial work on ligands for hydroformylation carried out by Shell in the 1960s focused on tri-*n*-butylphosphine,[9] but

* Authors to whom correspondence should be addressed. E-mail: wolfgang.meyer@sasol.com (W.H.M.); cathy.dwyer@sasol.com (C.L.D.). Fax: +27-11-5222034. Tel: +27-16-9604715.
† Sasol Technology Research & Development.
‡ Sasol Technology (UK) Limited.

(1) (a) Ivin, K. J.; Mol, J. C. *Olefin Metathesis and Metathesis Polymerization*; Academic Press: London, 1997. (b) Fürstner, A. *Angew. Chem., Int. Ed.* **2000**, *39*, 3012. (c) Grubbs, R. H., Ed. *Handbook of Metathesis*; Wiley-VCH: Weinheim, Germany, 2003; Vols. 1−3. (d) Grubbs, R. H. *Tetrahedron* **2004**, *60*, 7117.

(2) Pederson, R. L. Commercial Applications of Ruthenium Metathesis Processes. In *Handbook of Metathesis*; Grubbs, R. H., Ed.; Wiley-VCH: Weinheim, Germany, 2003; Vol. 2, p 491.

(3) (a) Weskamp, T.; Schattenmann, W. C.; Speigler, M.; Herrmann, W. A. *Angew. Chem., Int. Ed.* **1998**, *37*, 2490. (b) Ackermann, L.; Fürstner, A.; Weskamp, T.; Kohl, F. J.; Herrmann, W. A. *Tetrahedron Lett.* **1999**, *40*, 4787. (c) Weskamp, T.; Kohl, F. J.; Herrmann, W. A. *J. Organomet. Chem.* **1999**, *582*, 362. (d) Frenzel, U.; Weskamp, T.; Kohl, F. J.; Schattenmann, W. C.; Nuyken, O.; Herrmann, W. A. *J. Organomet. Chem.* **1999**, *586*, 263. (e) Scholl, M.; Trnka, T. M.; Morgan, J. P.; Grubbs, R. H. *Tetrahedron Lett.* **1999**, *40*, 2247. (f) Jafarpour, L.; Huang, J.; Stevens, E. D.; Nolan, S. P. *Organometallics* **1999**, *18*, 3760. (g) Scholl, M.; Ding, S.; Lee, C. W.; Grubbs, R. H. *Org. Lett.* **1999**, *1*, 953. (h) Huang, J.; Stevens, E. D.; Nolan, S. P.; Peterson, J. L. *J. Am. Chem. Soc.* **1999**, *121*, 2674. (i) Weskamp, T.; Kohl, F. J.; Hieringer, W.; Gleich, D.; Herrmann, W. A. *Angew. Chem., Int. Ed.* **1999**, *38*, 2416. (j) Sanford, M. S.; Love, J. A.; Grubbs, R. H. *J. Am. Chem. Soc.* **2001**, *123*, 6543.

(4) (a) Janse van Rensburg, W.; Steynberg, P. J.; Meyer, W. H.; Kirk, M. M.; Forman, G. S. *J. Am. Chem. Soc.* **2004**, *126*, 14332. (b) Amoroso, D.; Yap, G. P. A.; Fogg, D. E. *Organometallics* **2002**, *21*, 3335. (c) Trnka, T. M.; Morgan, J. P.; Sanford, M. S.; Wilhelm, T. E.; Scholl, M.; Choi, T.-L.; Ding, S.; Day, M. W.; Grubbs, R. H. *J. Am. Chem. Soc.* **2003**, *125*, 2546.

(5) (a) Nolan, S. P. *J. Organomet. Chem.* **2002**, *643*−*644*, 247. (b) Dinger, M. B.; Mol, J. C. *Organometallics* **2003**, *22*, 1089. (c) Dinger, M. B.; Mol, J. C. *Eur. J. Inorg. Chem.* **2003**, 2827. (d) Lehman, S. E.; Schwenderman, J. E.; O'Donnell, P. M.; Wagener, K. B. *Inorg. Chim. Acta* **2003,** *345*, 190.

(6) (a) Dinger, M. B.; Mol, J. C. *Adv. Synth. Catal.* **2002**, *344*, 671. (b) Dinger, M. B.; Nieczypor, P.; Mol, J. C. *Organometallics* **2003**, *22*, 5291.

(7) Grubbs, R. H. *Angew. Chem., Int. Ed. Engl.* **1995**, *34*, 2039.

10.1021/om051079p CCC: $33.50
Publication on Web 06/16/2006

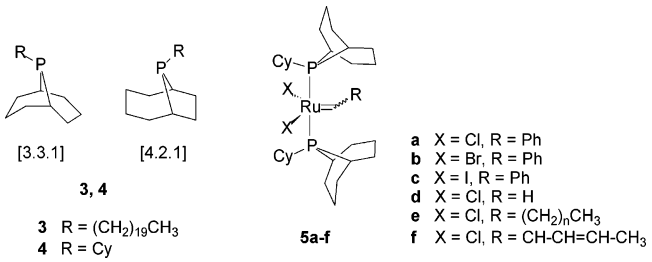

Figure 2. Phoban ligands **3** and **4**, showing structural isomers present in the mixture, and phobcat-type catalysts **5a**−**f**.

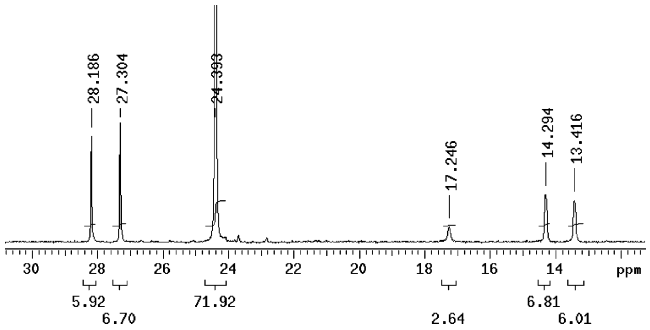

Figure 3. ^{31}P NMR spectrum of phobcat (**5a**) at −40 °C ($CDCl_3$).

further research led them to the development and commercialization of catalysts based on 9-phosphabicyclononane ("phoban") derived ligands, specifically eicosylphoban (**3**) (Figure 2).[10] Here, the ruthenium alkylidene complex **5a** ("phobcat") bearing cyclohexylphoban (**4**) as ligands shows superior performance in cross-metathesis (CM) and ring-closing metathesis (RCM) with respect to improved catalyst stability and good selectivity to primary metathesis products.[11] Recent synthetic studies and spectroscopic investigations have revealed an interesting conformational behavior of **5**, which may be relevant to catalytic performance and the further development of such systems. These studies will be discussed in more detail below.

Results and Discussion

The cyclohexylphoban benzylidene precatalyst **5a** was previously characterized at room temperature by ^{31}P NMR, showing a broad singlet at 23.3 ppm.[11] The broadness of the peak was initially ascribed to slow ligand exchange. In ^{31}P NMR at −40 °C, however, a number of sharp peaks were obtained for **5a** in $CDCl_3$ instead of the expected sharp singlet: one singlet at δ 24.4 ppm, two doublets at δ 27.7 and 13.9 ppm (both with J = 214 Hz and integrating for equivalent values), and a further singlet at δ 17.2 ppm (Figure 3). A ^{31}P−^{31}P COSY experiment revealed that the two doublets were coupled, confirming that they represented two nonequivalent phosphines on a single ruthenium center.[12] In ^{1}H NMR two major carbene peaks were

Scheme 1. Synthesis of Ligands and Phobcat

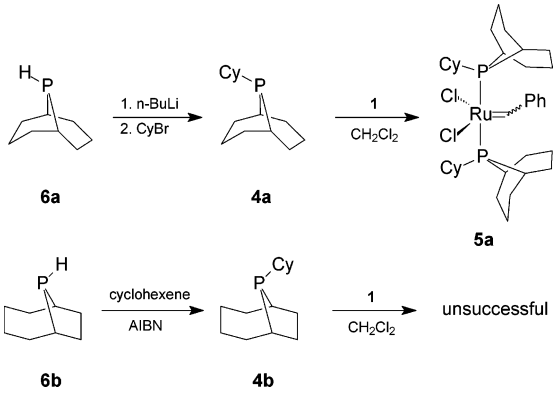

observed in $CDCl_3$,[12] but there were three peaks in toluene-d_8 which correlated (by integration and ^{1}H−^{31}P HMBC) to the three species seen in the ^{31}P NMR.

This information suggested we were dealing with a mixture of at least three discrete ruthenium carbene species in solution, two resonating as singlets (equivalent phosphines) and one resonating as two coupled doublets (two nonequivalent phosphines). In the solid state, however, only one structure was found for the similar butenylidene complex **5f**.[11] A change in the concentration of the complex did not alter the peak ratio in further ^{31}P NMR experiments, so that a monomer−dimer equilibrium or similar process could be ruled out. Other possibilities of the species in equilibrium include cis/trans isomers and rotational isomers, if the phosphine rotation is restricted. Since a mixture of the [3.3.1]- and [4.2.1] cyclohexylphoban isomer is used in the synthesis of complex **5a**, the possibility of mixed and ligand exchanging complex had to be considered as well. Such mixed complexes are known e.g. for dimeric cobalt carbonyl complexes.[13]

Phoban Structural Isomers. To assess the possibility of incorporation of the [4.2.1] isomer, the synthesis of the pure cyclohexyl-[3.3.1]-phoban isomer was undertaken. This involved separation of a commercial phoban [3.3.1]/[4.2.1] mixture (**6a**/**6b** in ratio of 1.2/1) using the method of Pringle and coworkers.[14]

Since the radical addition of **6a** to cyclohexene was not successful, **6a** was reacted with *n*-BuLi followed by cyclohexyl bromide (Scheme 1). The cyclohexyl-[3.3.1]-phoban ligand (**4a**) was obtained after purification in a yield of 32%. Reaction of **4a** with **1** proceeded smoothly in DCM to afford **5a** in respectable yield. However, ^{31}P NMR of the product at −40 °C afforded a spectrum identical with that obtained with the catalyst prepared from the ligand mixture (Figure 3), which confirms that the complex NMR spectra reported above did not result from the incorporation of the [4.2.1] isomer. To add further weight to this, we attemped to synthesize the ruthenium complex containing the [4.2.1] isomer. Radical addition of **6b** to cyclohexene produced **4b**, but further reaction with **1** was unsuccessful. The found incapability of cyclohexyl-[4.2.1]-phoban to displace tricyclohexylphosphine confirms the possible application of the [3.3.1]/[4.2.1] mixture for the synthesis of the ruthenium complex **5a**.

Cis−Trans Isomerization. The possibility of cis and trans complexes arising from orientation of the phosphines was considered. The existence of such isomers has been reported, for example, for the osmium carbonyl carbene complex [Os-

(8) (a) Crause, C.; Bennie, L.; Damoense, L.; Dwyer, C. L.; Grove, C.; Grimmer, N.; Janse van Rensburg, W.; Kirk, M. M.; Mokeseng, K.; Otto, S.; Steynberg, P. J. *Dalton Trans.* **2003**, 2036. (b) Dwyer, C. L.; Assumption, H.; Coetzee, J.; Crause, C.; Damoense, L.; Kirk, M. M. *Coord. Chem. Rev.* **2004**, *248*, 653.

(9) (a) Slaugh, L. H.; Mullineaux, R. D. *J. Organomet. Chem.* **1968**, *13*, 469. (b) Slaugh, L. H.; Mullineaux, R. D. U.S. Patent 3,239,569, 1968.

(10) Mason, R. F.; van Winkle, J. L. U.S. Patent 3,400,163, 1968.

(11) (a) Forman, G. S.; McConnell, A. E.; Hanton, M. J.; Slawin, A. M. Z.; Tooze, R. P.; Janse van Rensburg, W.; Meyer, W. H.; Dwyer, C. L.; Kirk, M. M. Serfontein, D. W. *Organometallics* **2004**, *23*, 4824. (b) Forman, G. S.; McConnell, A. E.; Tooze, R. P.; Dwyer, C.; Serfontein, D. W. (Sasol Technology UK) World Patent ZA03/00087, 2003.

(12) See the Supporting Information.

(13) Otto, F. Personal communication.

(14) Downing, J. H.; Gee, V.; Pringle, P. G. *J. Chem. Soc., Chem. Commun.* **1997**, 1527.

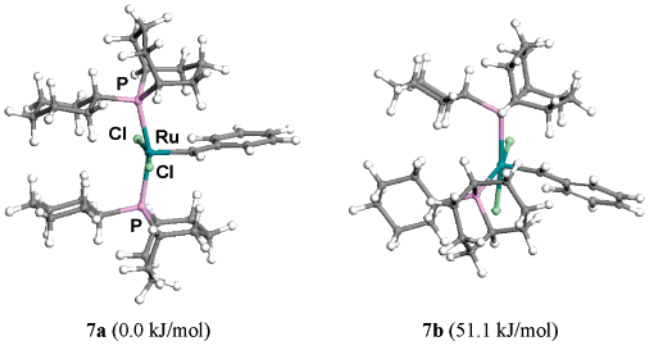

Figure 4. Optimized geometries of the lowest energy trans (**7a**)- and cis complexes (**7b**) of the phoban-derived catalyst **5a**.

$(P^iPr_3)_2Cl_2(CO)(=CHPh)]$,[15] but with respect to the orientation of the smaller chlorine ligands, while the coordinated phosphines remained in a trans orientation. No cis−trans isomerism of the coordinated phosphines has been reported for Grubbs first-generation catalysts. To assess the probability of such isomerism in **5a**, high-level density functional theory (DFT) calculations were performed to determine the energy differences between the lowest energy trans and cis complexes, illustrated as **7a** and **7b** in Figure 4, respectively. From the calculations it is found that the cis complex (**7b**) is 51.1 kJ/mol higher in energy compared to the trans complex, effectively suggesting that cis−trans isomerization is highly unlikely to account for the observed ^{31}P NMR data. The high relative energy of **7b** is attributed to steric congestion between the two ligands, as is evident from the P−Ru−P angle of 105.1°, which deviates significantly from the ideal 90° angle. Further evidence in favor of the trans complex **7a** is the observed coupling constant of the species resonating as a doublet ($J = \sim 210$ Hz), which is more typical of trans complexes.[16]

Rotational Isomerism. The hindered rotation about a metal−phosphorus bond has been reported, for example, for complexes of palladium,[17a] iron,[17b−d] molybdenum and tungsten,[17e] and rhodium[17f,g] as well as for ruthenium.[17h] After an early report[17i] on rotational isomerism in solution of iron piano-stool complexes with nonsymmetric silyl ligands evidenced by infrared spectroscopy, the same phenomenon was observed for similar iron complexes with dimethylphenylphosphine or methyldiphenylphosphine as ligand using a combination of infrared and NMR techniques.[17d] In ruthenium chemistry, the complex $[RuCl_2(triphos)_2]$ (triphos = $(Ph_2P(CH_2)_2)_2PPh$) is an example of rotational isomerism due to two different orientations of one triphos ligand bound only via the central phosphorus atom to the metal center, as indicated by a split in the corresponding phosphorus signals in ^{31}P NMR at −75 °C.[17h] To the best of our knowledge, rotational isomerism for ruthenium alkylidene complexes bearing phosphines of low symmetry ($< C_3$) has not been reported: the complexes $[RuL_2X_2(=CHCH=CPh_2)]$[18a] (L = PCy_2Ph, P^iPr_2Ph; X = Cl, Br, I), $[Ru(Cy_2PCH_2CH_2N(CH_3)_3^+Cl^-)_2Cl_2(=CHPh)]$,[18b,c] and $[Ru(Cy_2PCH_2Si(CH_3)_3)_2Cl_2(=CHPh)]$[18d] did not exhibit any unusual spectroscopic behavior at room temperature which otherwise might have prompted further studies into the potential rotational isomerism of these compounds. For the last complex, however, the authors describe in the metathesis of a norbornene imide two overlapping doublet signals for the carbene proton in the ^{1}H NMR, which indicate the existence of two different propagating species bearing one phosphine ligand. This is not attributed to a cis or trans configuration of the last inserted monomer but rather to the possible existence of rotameric isomers, which remain to be identified.[18d]

Scheme 2. Different Rotamer Structures of Phobcat (5a)

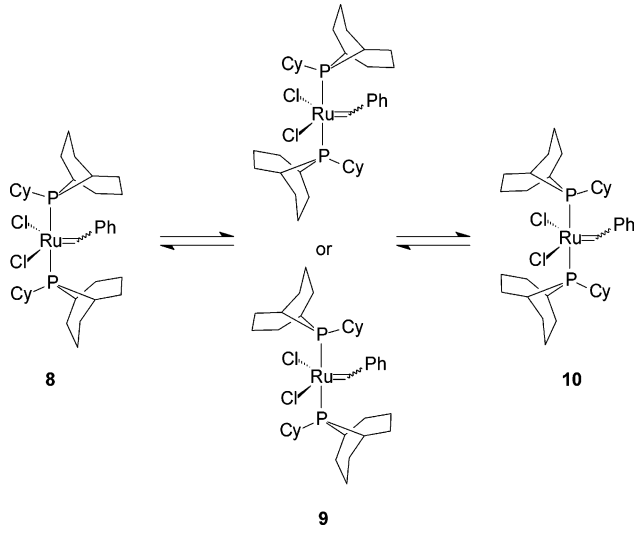

Concerning rotation about the Ru−P bond, there are three possibilities for rotational isomers for **5a**, which can be defined by the orientation of the cyclohexyl rings with respect to the benzylidene moiety: (i) both cyclohexyl rings transoid (**8**), (ii) one cyclohexyl ring transoid and the other cisoid (**9**, two mirror-image structures), and (iii) both cyclohexyl fragments cisoid to the benzylidene moiety (**10**) (Scheme 2). The number of isomers matches that seen in the NMR spectra and would also account for the coupling pattern observed in the ^{31}P NMR (two species with equivalent phosphines, and one species with nonequivalent phosphines).

Isomer **8** corresponds to the phobcat butenylidene crystal structure obtained previously[11] and on this basis would be expected to be the lowest energy conformer. The DFT-optimized geometries and relative energies (kJ/mol) of **8**−**10** are summarized in Figure 5 and confirm the relative stability of **8**.

The energy of **9** is calculated to be 3.0 kJ/mol higher than for **8**. This predicted energy difference is in excellent agreement with the experimental difference in energies obtained between the two highest concentration structures in the ^{31}P and ^{1}H NMR analyses (3.6 kJ/mol).[12] The rotational isomer **10** is calculated to be higher in energy than **8** by 9.3 kJ/mol. An additional rotational isomer was optimized in which the bottom cyclohexylphoban ligand in **8** was oriented along the Cl−Ru−Cl axis. This geometry (**11**), with a $C_{carbene}-Ru-P_{bottom}-C_{Cy}$ dihedral

(15) Werner, H.; Stüer, W.; Laubender, M.; Lehmann, C.; Herbst-Irmer, R. *Organometallics* **1997**, *16*, 2236.

(16) Berger, S.; Braun, S.; Kalinowski, H. *NMR Spectroscopy of the Nonmetallic Elements*; Wiley: New York, 1997; pp 954−959.

(17) (a) Albert, J.; Bosque, R.; Cadena, J. M.; Delgado, S.; Granell, J. *J. Organomet. Chem.* **2001**, *634*, 83. (b) Nakazawa, H. *J. Organomet. Chem.* **2000**, *611*, 349. (c) Girard, L.; Baird, M. C. *J. Organomet. Chem.* **1993**, *444*, 143. (d) Faller, J. W.; Johnson, B. V. *J. Organomet. Chem.* **1975**, *96*, 99. (e) Bennett, M. A.; Tomkins, I. B. *J. Organomet. Chem.* **1973**, *51*, 289. (f) Asaro, F.; Garlatti, R. D.; Pellizer, G.; Tauzher, G. *Inorg. Chim. Acta* **1993**, *211*, 27. (g) Topping, R. J.; Quin, L. D.; Crumbliss, A. L. *J. Organomet. Chem.* **1990**, *385*, 131. (h) Guimerans, R. R.; Hernandez, E. C.; Olmstead, M. M.; Balch, A. L. *Inorg. Chim. Acta* **1989**, *165*, 45. (i) Jetz, W.; Graham, W. A. G. *J. Am. Chem. Soc.* **1967**, *89*, 2773.

(18) (a) Dias, E. L.; Nguyen, S. T.; Grubbs, R. H. *J. Am. Chem. Soc.* **1997**, *119*, 3887. (b) Mohr, B.; Lynn, D. M.; Grubbs, R. H. *Organometallics* **1996**, *15*, 4317. (c) Lynn, D. M.; Mohr, B.; Grubbs, R. H.; Henling, L. M.; Day, M. W. *J. Am. Chem. Soc.* **2000**, *122*, 6601. (d) Robson, D. A.; Gibson, V. C.; Davies, R. G.; North, M. *Macromolecules* **1999**, *32*, 6371.

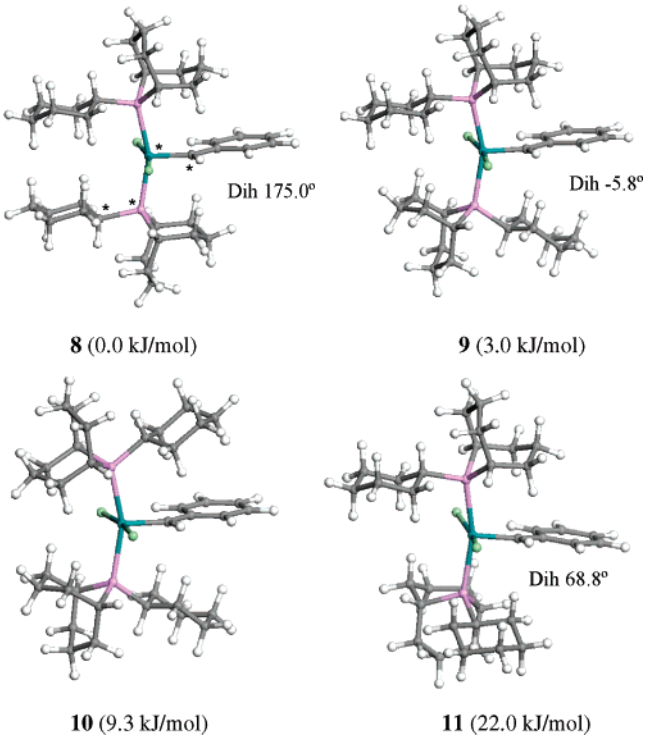

Figure 5. Relative energies and optimized structures for rotational isomers of the phoban-derived catalyst **5a**.

angle of 68.8°, is illustrated along with that of **8** ($C_{carbene}-Ru-P_{bottom}-C_{Cy} = 175.0°$) in Figure 5. The relatively high energy of **11** (22.0 kJ/mol) suggests that rotational isomers resembling **11** would be unlikely to be detected on the NMR time scale. Together with the spectroscopic evidence, these results substantiate the presumed rotational isomerism and allow the assignment of the conformers to the signals in the ^{31}P NMR spectrum at low temperatures.

In an effort to further investigate the potential energy surface (PES) for rotational isomerism of **5a**, calculations were conducted[19] on a series of structures of which the dihedral angle of $C_{carbene}-Ru-P_{bottom}-C_{Cy}$ in **8** was incrementally changed by 20° to complete a full rotation of the lower cyclohexylphoban ligand through 360°. Only the scenario for rotation of one ligand was considered. The top cyclohexylphoban ligand was left unchanged (and unconstrained) along the transoid $P-Cy/C_{carbene}$ orientation. This PES estimate is graphically illustrated in Figure 6.

It is evident that four energy minima may be identified when only one of the two cyclohexylphoban ligands is rotated. The lowest energy structure corresponds to **8** (dihedral angle 175.0°; 0.0 kJ/mol), while the second lowest energy geometry corresponds to structure **9** (dihedral angle −5.8°; 3.0 kJ/mol). Two additional local minima are located at dihedral angles of 68.8° (22.0 kJ/mol, **11**) and −100.1° (26.0 kJ/mol). The last two structures are high-energy local minima on the PES corresponding to structures in which the rotating ligand is oriented parallel to the Cl−Ru−Cl axis and should not be detectable via NMR, due to the low barriers needed to convert to true minima structures. The two true minima on the PES (**8** and **9**), however, need relatively high energies to interconvert, i.e. 30.5 kJ/mol (dihedral angle −80.2°) and 33.2 kJ/mol (dihedral angle 100.0°), depending on the direction of rotation of the rotating ligand. These relatively high estimated activation barriers explain why it is possible to detect the different isomeric species by NMR at low temperatures, effectively freezing out the isomeric species in the low-energy basins.

Given that the above calculations indicate that steric factors should influence the barriers to rotation, additional complexes were synthesized to further corroborate the existence of rotational isomers: a less sterically encumbered phobcat methylidene species (**5d**) was prepared by reaction of **5a** with ethylene, and the more sterically encumbered phobcat bromide (**5b**) and iodide (**5c**) were prepared from **5a** via halogen exchange.

The optimized structures and relative energies of the three lowest energy phobcat methylidene rotamers were calculated by DFT, and the results are summarized in Table 1. It is clear that the reduced steric bulk of the small and symmetrical methylidene compared to the bulkier benzylidene results in smaller energy differences for the different conformers, which is experimentally reflected in a more even distribution of the rotamers (Table 1). Furthermore, as the barrier to rotation is lowered, rotation of the ligands is speeded up; thus, peaks should still be very broad at room temperature. Both of these trends are observed.

With their bulkier halogenide ligands, phobcat bromide (**5b**) and phobcat iodide (**5c**) should exhibit an increasing barrier for the phosphine rotation and therefore show slower rotation, which should lead to sharper NMR resonances at higher temperatures. Indeed, while **5a** gives usable spectra with good resolution at and below −20 °C, **5b** gives sharp peaks at 0 °C, only becoming broad above 30 °C, at which temperature **5c** still shows sharp peaks (Figure 7).

The coupling constant obtained for the two ^{31}P nuclei on the asymmetrical isomer gives an indication of the Ru−P bond length for comparison purposes.[16] It is expected that the Ru−P bond length will increase as the chloride ligand is replaced with the bulkier bromide and iodide ligands, resulting in a decrease in the coupling constant.[20] This trend is observed for the phobcat halogenides (Table 2). At the same time, the P−Ru−P angle remains almost unchanged, so that the influence of this bond angle on the coupling constant can be excluded. The phobcat methylidene complex cannot be included in the comparison, due to its different alkylidene moiety.

Finally, rotational isomerism provides the answer to an additional observation: phobcat benzylidene (**5a**) shows an unusual pattern in the aromatic region of the ^1H NMR spectrum. Four broad singlet signals were found at room temperature integrating in a ratio of 1:1:1:2. In contrast, for the Grubbs catalyst one observes three sharper signals integrating for 2:1:2 at room temperature and four signals in a 1:1:1:2 ratio at −60 °C. The low-field signal at δ 9.3 ppm of **5a** splits into two signals with an integration ratio of 3:7 at −40 °C (Figure 8). A less pronounced split can be observed for the signal at δ 7.9 ppm. The pattern of these ^1H NMR signals can be explained by considering two inequivalent ortho H atoms on the NMR time scale which experience a further differentiation at low temperatures due to another set of different chemical environments for the ortho H atom. A hindrance of the rotation of the phenyl group must be the prerequisite for such an observation, which becomes apparent at −40 °C for **5a** and at −60 °C for the Grubbs catalyst. As a tentative assignment the ortho H closest to the carbene proton (cisoid) shows a ^1H signal about δ 9.3 ppm at room temperature, whereas the signal of the second ortho H (transoid) is found at δ 7.9 ppm. At −40 °C the two previously mentioned major carbene species of **5a** show not only two different carbene H signals but also two different signals of the cisoid ortho H (δ 9.42 and 9.22 ppm) and transoid ortho H (δ 7.95 and 7.91

(19) COARSE convergence criteria were used for these calculations; see Computational Details in the Experimental Section.

(20) Verkade, J. G. *Coord. Chem. Rev.* **1972**, *9*, 1.

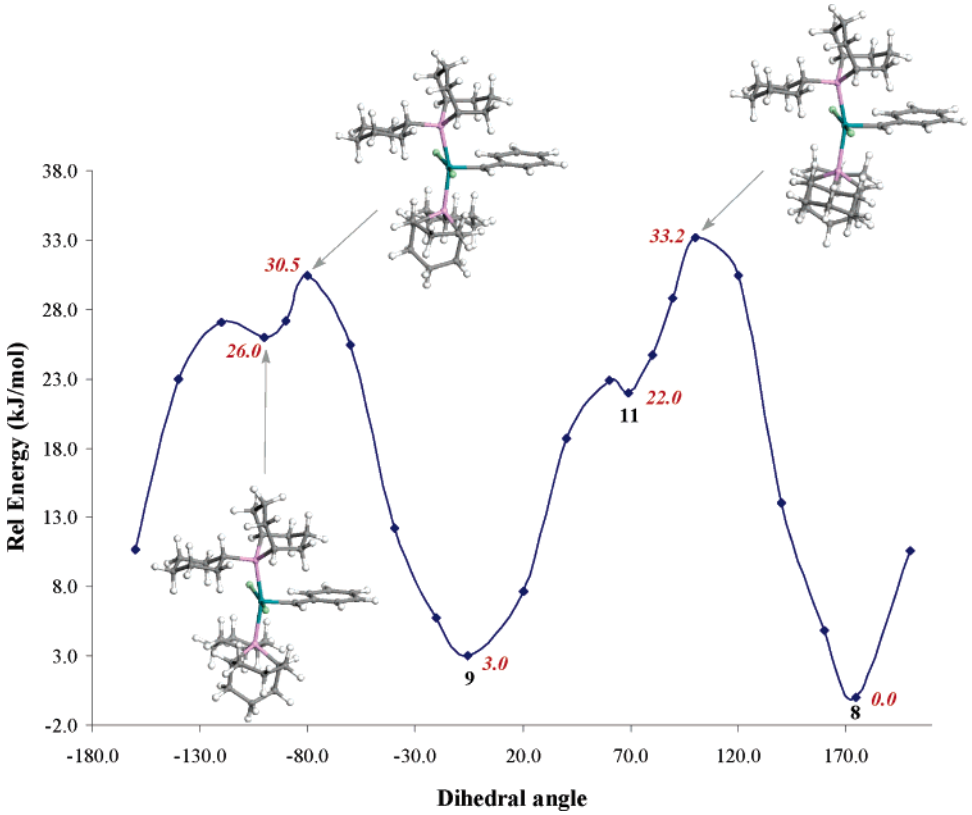

Figure 6. Potential energy surface for rotation of the lower cyclohexylphoban ligand.

Table 1. Comparison of Experimentally Determined (^{31}P NMR, $CDCl_3$, − 40 °C) Abundance versus Relative DFT-Calculated Energies for the Three Lowest Energy Rotamers of 5a−d

	conformation type **8**		conformation type **9**		conformation type **10**	
complex	^{31}P NMR (mol % P)	calcd rel energy (kJ/mol)	^{31}P NMR (mol % P)	calcd rel energy (kJ/mol)	^{31}P NMR (mol % P)	calcd rel energy (kJ/mol)
phobcat (**5a**)	69	0.00	28	3.0	3	9.3
phobcat bromide (**5b**)[a]	84	0.00	15	5.1	1	13.6
phobcat iodide (**5c**)[a]	86	0.00	14	8.3	not detected	19.7
phobcat methylidene (**5d**)[a]	37	0.00	45	2.0	18	5.7

[a] Similar ligand orientations compared to **5a**; structure coordinates included in the Supporting Information.

ppm). The integration of the split signals correlates with the ratios found from the carbene H and the results from the ^{31}P NMR studies. Further investigations into the rotational behavior of the carbene groups are underway.

Conclusions

The new metathesis catalysts based on phoban ligands show interesting solution behavior, where the bulky phoban cannot rotate freely around the P−Ru−P axis due to interference from the equatorial halide and alkylidene groups. This gives rise to discrete rotational isomers, which can be seen clearly at low temperatures using ^{1}H and ^{31}P NMR. In addition, DFT evaluation of the rotational isomers provides for important corroborative elucidation of the spectroscopic data.

Previous[11] and current experimental evaluations of these catalysts have confirmed the superior catalytic performance of phoban-derived Grubbs catalyst analogues relative to that of the commercial PCy_3-based catalyst. Current studies are focusing on understanding whether the conformational behavior of the phoban catalysts is linked to the observed superior activity and stability of such catalysts. The difference in ligand rotation during the swing mechanism of the metathesis mechanistic cycle for Grubbs first- (**1**) and second-generation (**2**) catalysts was pointed out by Chen et al. as a result of DFT studies: while the PCy_3 ligand in the ruthenacyclobutane structure rotates 120° during catalysis with **1** to allow productive metathesis, the IMes ligand in **2** does not rotate to gain a lower energy structure.[21] Likewise, no rotation of the ligand in phobcat is necessary on energetic grounds.

Experimental Section

NMR Analysis. NMR samples were handled under argon. NMR spectra were recorded on a Bruker 500 MHz NMR spectrometer fitted with a QNP 5 mm probe or a Varian 600 MHz NMR spectrometer fitted with a switchable 5 mm pfg probe. Spectra were carried out at −40 °C (unless stated otherwise) using either $CDCl_3$ or toluene-d_8 as a lock solvent. For the 1D ^{31}P spectra, at least 256 scans were recorded with a 30° pulse angle using the zg30 pulse sequence or the s2pul sequence. For the ^{1}H spectra, at least 32 scans were recorded with a 30° pulse angle using the zg30 or s2pul pulse sequence.

The ^{31}P−^{31}P COSY spectra were carried out using a modified version of the Bruker ^{1}H−^{1}H COSY pulse sequence with gradients,

(21) Adlhart, C.; Chen, P. *Angew. Chem., Int. Ed.* **2002**, *41*, 4484.

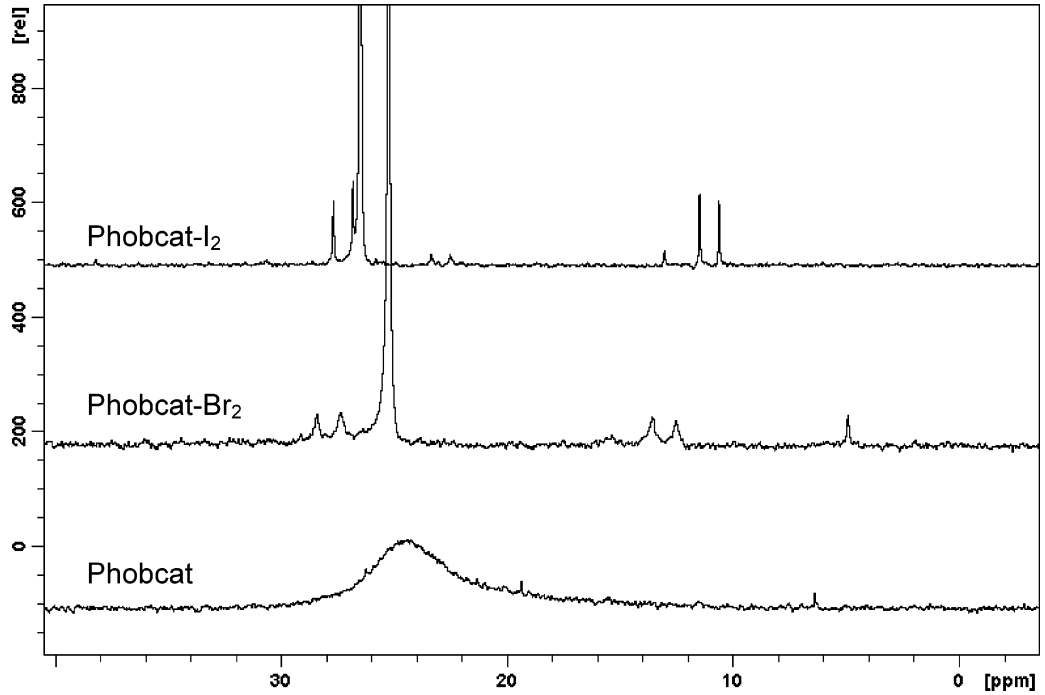

Figure 7. ^{31}P NMR spectra of phobcat, phobcat bromide, and phobcat iodide (**5a**−**c**) at 30 °C.

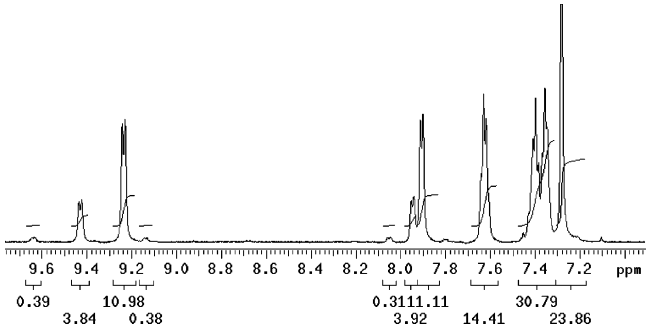

Figure 8. Aromatic region of ^{1}H NMR of phobcat (**5a**) at −40 °C.

Table 2. ^{31}P Coupling Constants and DFT-Calculated Ru−P Bond Lengths and P−Ru−P Bond Angles for Different phobcat-Type Complexes

complex	$^{2}J_{PP}$ (Hz)	Ru−P (Å)	P−Ru−P (deg)
phobcat (**5a**)	214	2.445	159.6
phobcat bromide (**5b**)	210	2.453	159.3
phobcat iodide (**5c**)	207	2.468	159.2
phobcat methylidene (**5d**)	204	2.434	161.8

cosydcph. The F1 nucleus was changed to ^{31}P, and ^{1}H decoupling was introduced. The number of increments was set to 128, with 4 scans per increment, and a 2 s relaxation delay was used. The ^{31}P−^{1}H HMBC spectra were carried out using a modified version of the ^{13}C−^{1}H HMBC with gradients, inv4gplrndqf. The F1 nucleus was changed to ^{31}P. The number of increments was set to 256, with 4 scans per increment, and a 1.5 s relaxation delay was used.

Computational Details. All equilibrium geometry optimizations were performed with the DMol^{3} density functional theory (DFT) code[22] as implemented in the MaterialsStudio (Version 3.2) program package of Accelrys Inc. The nonlocal generalized gradient approximation (GGA) exchange correlation functional by Perdew and Wang (PW91)[23] was used for all calculations. DMol^{3} utilizes a basis set of numeric atomic functions, which are exact solutions of the Kohn−Sham equations for the atoms.[24] These basis sets are generally more complete than a comparable set of linearly independent Gaussian functions and have been demonstrated to have small basis set superposition errors.[24] In the present work a polarized split valence basis set, termed a double numeric polarized (DNP) basis set, has been used. All geometry optimizations employed highly efficient delocalized internal coordinates.[25]

Two sets of convergence criteria were used for geometry optimizations: the first set of convergence criteria (denoted as FINE convergence) was used for most geometry optimizations and consisted of threshold values of 2×10^{-5} hartree, 0.00189 hartree/Å, and 0.00529 Å for energy, gradient, and displacement convergence, respectively, while a self-consistent-field (SCF) density convergence threshold value of 1×10^{-6} hartree was specified. The second set of convergence criteria (denoted as COARSE convergence) were used for the constrained geometry optimizations for ligand rotation at specified $C_{carbene}-Ru-P_{bottom}-C_{Cy}$ dihedral angles and consisted of threshold values of 1×10^{-4} hartree, 0.02 hartree/Å, and 0.05 Å for energy, gradient, and displacement convergence, respectively, while a SCF convergence of 1×10^{-4} hartree was specified. All calculated energies are electronic energies without the incorporation of zero-point energy (ZPE) and entropy corrections. This approach is motivated by the fact that the energies of isomers of a single unimolecular molecule, without change in nature or number of atoms, are compared, for which negligible relative entropy corrections are anticipated.

Synthesis. Lithium bromide (Aldrich), sodium iodide (Aldrich), cyclohexyl bromide (Aldrich), *n*-butyllithium solution (1.6 M in *n*-hexane; Aldrich), and Grubbs catalyst (Fluka) were used without further purification. All solvents were dried and deoxygenated using common laboratory procedures.

Phobcat (benzylidenedichlorobis(9-cyclohexyl-9-phosphabicyclo-[3.3.1]-nonane)ruthenium, **5a**) was synthesized via ligand exchange starting from Grubbs catalyst and an excess of either a mixture of cyclohexyl-[3.3.1]-phoban (9-cyclohexyl-9-phosphabicyclo-[3.3.1]-nonane) and cyclohexyl-[4.2.1]-phoban or the pure [3.3.1] isomer.

(22) (a) Delley, B. *J. Chem. Phys.* **1990**, *92*, 508. (b) Delley, B. *J. Phys. Chem.* **1996**, *100*, 6107. (c) Delley, B. *J. Chem. Phys.* **2000**, *113*, 7756.

(23) Perdew, J. P.; Wang, Y. *Phys. Rev.* **1992**, *B45*, 13244.

(24) Delley, B. In *Density Functional Theory: A Tool for Chemistry*; Seminario, J. M., Politzer, P., Eds.; Elsevier: Amsterdam, The Netherlands, 1995.

(25) Andzelm, J.; King-Smith, R. D.; Fitzgerald, G. *Chem. Phys. Lett.* **2001**, *335*, 321.

The synthesis and characterization at room temperature as well as the synthesis and characterization of methylidenedichlorobis(9-cyclohexyl-9-phosphabicyclo-[3.3.1]-nonane)ruthenium (**5d**) have been described elsewhere.[11]

The [3.3.1]/[4.2.1] mixture of phosphabicyclononane was separated using a published procedure.[14]

9-Cyclohexyl-9-phosphabicyclo-[3.3.1]-nonane (4a). 9-Phosphabicyclo[3.3.1]nonane (4.2 g, 29.5 mmol) was dissolved in diethyl ether (100 mL). After this solution was cooled to −30 °C, a solution of *n*-butyllithium in hexane (1.6 M, 20.3 mL, 32.5 mmol) was added with stirring over 10 min at this temperature. The reaction mixture was warmed to room temperature within 60 min and then cooled to 0 °C. Cyclohexyl bromide (4.0 mL, 32.5 mmol) was added over 5 min to the stirred mixture. The cooling bath was removed, and the reaction mixture was stirred overnight. ^{31}P NMR of the reaction mixture showed formation of the product in about 45% yield. The major product (50% yield) produced a singlet at δ −46 ppm in ^{31}P NMR and is believed to be a dimeric compound with a P−P bond. The solvent was removed in vacuo and the residue subjected to a Kugelrohr distillation at 0.8×10^{-2} mbar. The product was collected between 115 and 140 °C as a white solid (2.1 g, 32%). ^{1}H NMR ($CDCl_3$, 400 MHz, 303 K): δ 3.48 (m, 1H), 2.2−0.9 (m, 24H). ^{31}P{^{1}H} NMR ($CDCl_3$, 162 MHz, 303 K): δ −24.9 (s). MS (main peaks): *m*/*z* 224 (M^+, 62%), 142 (38%).

9-Cyclohexyl-9-phosphabicyclo-[4.2.1]-nonane (4b). 9-Phosphabicyclo-[4.2.1]-nonane (1.1 g, 7.7 mmol) and 6 mL of cyclohexene were heated to 90 °C in the presence of 100 mg of AIBN (0.61 mmol). After 16 h reaction time, a conversion of 80% was achieved with the mixture containing 62% **4b** according to ^{31}P NMR. A further addition of 50 mg of AIBN (0.30 mmol) and 2 mL of cyclohexene was followed by the addition of the same amount after 8 h. The product mixture contained 79% **4b** and less than 4% of the phoban starting material after a further reaction time of 12 h according to ^{31}P NMR. The mixture was cooled, and the volatile components were removed in vacuo. The resulting light yellow oil was subjected to a Kugelrohr distillation at 0.8×10^{-2} mbar. The product was collected between 125 and 140 °C as a white solid (0.92 g, 53%). ^{1}H NMR ($CDCl_3$, 400 MHz, 303 K): δ 2.6−1.0 (m, 25H). ^{31}P{^{1}H} NMR ($CDCl_3$, 162 MHz, 303 K): δ 13.1 (s). MS (main peaks): *m*/*z* 224 (M^+, 36%), 142 (64%).

Phobcat Bromide (Benzylidenedibromobis(9-cyclohexyl-9-phosphabicyclo-[3.3.1]-nonane)ruthenium, 5b). Phobcat (450 mg, 0.633 mmol) and lithium bromide (1 g, 11.5 mmol) were stirred for 4 h in a mixture of tetrahydrofuran (5 mL) and dichloromethane (10 mL) at room temperature. The solvent was removed in vacuo and the residue dissolved in 5 mL of benzene. The suspension was centrifuged, and the lithium salts were separated from the solution via syringe. The solvent was removed in vacuo, and the exchange procedure was repeated with 1 g of lithium bromide overnight. The product was separated from the lithium salts via centrifugation. After removal of the solvent in vacuo the complex was washed once with 5 mL of cold pentane and then dried in vacuo. The complex was obtained as a dark violet powder (355 mg, 70%) and can be recrystallized from a 1:1 mixture of benzene and pentane at room temperature. Anal. Calcd for $C_{35}H_{56}Br_2P_2Ru$: C, 52.57; H, 7.06. Found: C, 52.96; H, 7.19. ^{1}H NMR ($CDCl_3$, 500 MHz, 303 K): δ 20.2−19.8 (m, br, 1H, C*H*Ph), 9.4 (s, br, 1H, ortho C_6H_5), 7.9 (s, br, 1H, ortho C_6H_5), 7.6 (m, 1H, para C_6H_5), 7.4 (m, 2H, meta C_6H_5), 3.6−0.5 (m, 50H, P ligand). ^{31}P{^{1}H} NMR ($CDCl_3$, 202.5 MHz, 303 K): δ 27.9 (d, $^2J_{PP}$ = 205 Hz, P^1 of nonsymmetric rotamer), 25.2 (s, main symmetric rotamer), 13.0 (d, $^2J_{PP}$ = 205 Hz, P^2 of nonsymmetric rotamer).

Phobcat Iodide (Benzylidenediiodobis(9-cyclohexyl-9-phosphabicyclo-[3.3.1]-nonane)ruthenium, 5c). Phobcat (450 mg, 0.633 mmol) and sodium iodide (1 g, 6.7 mmol) were stirred for 4 h in a mixture of tetrahydrofuran (5 mL) and dichloromethane (10 mL) at room temperature. The solvent was removed in vacuo, and the residue was dissolved in 5 mL of benzene. The supernatant solution was filtered through a Whatman syringe filter. The solvent was removed in vacuo, and the exchange procedure was repeated with 1 g of sodium iodide overnight. The product was separated from the sodium salts via filtration. After removal of the solvent in vacuo, the complex was washed once with 5 mL of cold pentane and then dried in vacuo. The complex was obtained as a green powder (232 mg, 41%) and can be recrystallized from a 1:1 mixture of benzene and pentane at room temperature. Anal. Calcd for $C_{35}H_{56}I_2P_2Ru$: C, 47.13; H, 6.33. Found: C, 47.49; H, 6.34. ^{1}H NMR (C_6D_6, 600 MHz, 303 K): δ 20.56 (s, br, 0.13H, C*H*Ph of nonsymmetric rotamer), 20.25 (s, br, 0.85H, C*H*Ph of main symmetric rotamer), 19.98 (s, br, 0.02H, C*H*Ph of minor symmetric rotamer), 8.7 (m, vbr, 1H, ortho C_6H_5), 7.3−7.0 (m, br, 4H, C_6H_5), 3.6−0.5 (m, 50H, P ligand). ^{31}P{^{1}H} NMR (C_6D_6, 242.8 MHz, 303 K): δ 26.8 (d, $^2J_{PP}$ = 207 Hz, P^1 of nonsymmetric rotamer), 25.9 (s, main symmetric rotamer), 12.6 (s, minor symmetric rotamer), 10.5 (d, $^2J_{PP}$ = 207 Hz, P^2 of nonsymmetric rotamer).

Acknowledgment. We thank Drs. Mike Green, Bob Tooze, and Petrie Steynberg for helpful discussions. We acknowledge Mr. Ivan Bester (Information Management, Sasol) for infrastructure support to the Sasol Molecular Modeling Group. We thank Sasol Technology Research and Development for permission to publish this work.

Supporting Information Available: Figures giving additional NMR spectra of **5a**, a table and van't Hoff plot for the determination of the energy differences of the rotamers, and tables giving the positions of atoms of the modeled complexes. This material is available free of charge via the Internet at http://pubs.acs.org.

OM051079P